Development 137, 2743-2752 (2010) doi:10.1242/dev.045872

Cytoskeletal dynamics and supracellular organisation of cell shape fluctuations during dorsal closure

Guy B. Blanchard[1,*], Sughashini Murugesu[1], Richard J. Adams[1], Alfonso Martinez-Arias[2] and Nicole Gorfinkiel[2,*]

SUMMARY

Fluctuations in the shape of amnioserosa (AS) cells during *Drosophila* dorsal closure (DC) provide an ideal system with which to understand contractile epithelia, both in terms of the cellular mechanisms and how tissue behaviour emerges from the activity of individual cells. Using quantitative image analysis we show that apical shape fluctuations are driven by the medial cytoskeleton, with periodic foci of contractile myosin and actin travelling across cell apices. Shape changes were mostly anisotropic and neighbouring cells were often, but transiently, organised into strings with parallel deformations. During the early stages of DC, shape fluctuations with long cycle lengths produced no net tissue contraction. Cycle lengths shortened with the onset of net tissue contraction, followed by a damping of fluctuation amplitude. Eventually, fluctuations became undetectable as AS cells contracted rapidly. These transitions were accompanied by an increase in apical myosin, both at cell-cell junctions and medially, the latter ultimately forming a coherent, but still dynamic, sheet across cells. Mutants with increased myosin activity or actin polymerisation exhibited precocious cell contraction through changes in the subcellular localisation of myosin. *thickveins* mutant embryos, which exhibited defects in the actin cable at the leading edge, showed similar timings of fluctuation damping to the wild type, suggesting that damping is an autonomous property of the AS. Our results suggest that cell shape fluctuations are a property of cells with low and increasing levels of apical myosin, and that medial and junctional myosin populations combine to contract AS cell apices and drive DC.

KEY WORDS: Cytoskeleton, Shape fluctuations, Morphogenesis, *Drosophila*

INTRODUCTION

The term morphogenesis refers to the dynamic reshaping of tissues that results in the stereotyped three-dimensional forms observed during embryonic development. Insight into the mechanics of morphogenetic processes is vital to understanding the construction of organs and tissues and to their assembly into organisms. However, as genetics and microscopy allow us to focus on single cells a paradox arises. Embryonic development is a reproducible deterministic process, but the individual cells that configure an organism exhibit remarkable behavioural heterogeneity when observed with enough time and spatial resolution (Blanchard et al., 2009; Martin et al., 2009; Mateus et al., 2009; Solon et al., 2009). How and when these heterogeneities are averaged into the stereotypical morphogenetic deformations are important questions of modern biology. The process of dorsal closure (DC) during *Drosophila* embryogenesis lends itself to quantifying behaviour at both the single-cell and tissue levels, and in combination with genetic perturbations provides a unique model with which to address the principles underlying averaging across length and time scales.

DC is a morphogenetic process that results in the closing of a gap that exists half way through embryogenesis in the dorsal epidermis (Harden, 2002; Jacinto and Martin, 2001; Martinez Arias, 1993). During DC, the epidermis elongates and converges towards the dorsal midline as the amnioserosa (AS) contracts and eventually disappears inside the embryo. DC is driven by forces generated by both epithelia and by their mechanical interactions (Gorfinkiel et al., 2009; Gorfinkiel and Martínez Arias, 2007; Grevengoed et al., 2001; Hutson et al., 2003; Kaltschmidt et al., 2002; Kiehart et al., 2000). The AS, in particular, provides much of the contractile force of DC (Franke et al., 2005; Kiehart et al., 2000; Lamka and Lipshitz, 1999; Scuderi and Letsou, 2005). We have previously shown that the contraction of the AS results from cell-autonomous apical contraction modulated by the mechanical constraints the tissue experiences (Gorfinkiel et al., 2009). In contrast to the collectively smooth movement of the whole tissue, individual AS cells display pulses of alternating contraction and expansion (Solon et al., 2009). These fluctuations are damped during DC, coincidentally with the appearance of a supracellular actin cable at the interface between the AS and the epidermis (Jacinto et al., 2002; Kiehart et al., 2000; Rodriguez-Diaz et al., 2008; Solon et al., 2009). This correlation has led to the proposal that the actin cable behaves as a ratchet, preventing expansion of fluctuating AS cells and promoting net cellular contraction of the tissue (Solon et al., 2009).

In the mesoderm of *Drosophila*, asynchronous pulsed apical contractions are associated with invagination and are correlated with bursts of apical actin-myosin accumulation, followed by a phase of stabilisation of the contracted state, and it has been suggested that the progressive enrichment of the actin-myosin apical meshwork acts as an intracellular ratchet to stabilise contractions (Martin et al., 2009). This actin-myosin meshwork forms a supracellular structure that allows the transmission of cellular forces to the whole tissue (Martin et al., 2010). The fluctuations that have been observed in the AS cells during DC provide another example of cellular dynamics associated with a

[1]Department of Physiology, Development and Neuroscience, University of Cambridge, Downing Street, Cambridge CB2 3DY, UK. [2]Department of Genetics, University of Cambridge, Downing Street, Cambridge CB2 3EH, UK.

*Authors for correspondence (gb288@cam.ac.uk; ng288@cam.ac.uk)

Accepted 9 June 2010

morphogenetic process and provide a good system with which to understand the molecular basis of the fluctuations and their role in the behaviour of sheets of cells. Here, we present a detailed quantitative analysis of AS cell fluctuations during DC and their relationship to the cytoskeleton.

MATERIALS AND METHODS

Drosophila strains

The following stocks were used: *ubiECad-GFP* (Oda and Tsukita, 2001), *Moe-GFP* (Edwards et al., 1997; Kiehart et al., 2000), *Spaghetti squash (Sqh)-GFP* (Royou et al., 2002), *Sqh-mCherry* (Martin et al., 2009), c381*Gal4* (an AS driver), *UAS-ctMLCK* [a constitutively active form of myosin light chain kinase (Kim et al., 2002)], *UAS-Dia^{CA}* [a constitutively active form of the formin Diaphanous (Somogyi and Rorth, 2004)] and *UAS-RhoN19* [a dominant-negative form of Rho (Strutt et al., 1997)]. *tkv^{8}* is an amorph allele for the Dpp receptor (García Fernández et al., 2007). UAS lines were expressed using the Gal4 system (Brand and Perrimon, 1993).

The following genotypes were analysed:
ubiECad-GFP;
sqh^{AX3}; Sqh-GFP;
Moe-GFP;
Moe-GFP; Sqh-mCherry;
ubiECad-GFP, Sqh-mCherry;
c381Gal4/ubiECad-GFP, Sqh-mCherry; UAS-ctMLCK;
c381Gal4/ubiECad-GFP, Sqh-mCherry; UAS-Dia^{CA};
c381Gal4/ubiECad-GFP, Sqh-mCherry; UAS-RhoN19;
tkv8, *ubiECad-GFP*.

Time-lapse movies

Stage 12-13 *Drosophila* embryos were dechorionated, mounted in coverslips with the dorsal side glued to the glass and covered with Voltalef oil 10S (Attachem). The AS was imaged at 24°C using an inverted LSM 510 Meta laser-scanning microscope with a 40× oil-immersion Plan/Fluor (NA 1.3) objective. The whole AS expressing ECad-GFP was imaged with an argon laser using the unmixing tool from the Zeiss software to remove autofluorescence from the vitelline membrane. Fifteen or sixteen *z*-sections 1.5 μm apart were collected every 30 seconds. GFP and mCherry cytoskeletal reporters were simultaneously imaged with an argon laser and a 561 nm diode laser and 5-6 *z*-sections 1 μm apart were collected every 10 seconds.

Immunostaining

Embryos were fixed and stained as described previously (Kaltschmidt et al., 2002). The following primary antibodies were used: rat monoclonal against *Drosophila* E-Cadherin, Shotgun (Dcad2, 1/20; Developmental Studies Hybridoma Bank, University of Iowa, developed by T. Uemura), rabbit antisera against phospho-Myosin light chain 2 (Cell Signaling). Alexa 488- and Alexa 647-conjugated antibodies (Molecular Probes) were used as secondary antibodies.

Cell tracking and data analysis

Cell shapes during DC were tracked from confocal stacks, projections of which are shown in Fig. 1A, as previously described (Blanchard et al., 2009; Gorfinkiel et al., 2009). Cell shape fluctuations were analysed using the cell radius time series of individual cells (Fig. 1B,C). Though initially we used cell area, we converted all area measures to radii [using radius=$\sqrt{}$(area/π)] because we considered that the actin-myosin contraction of cells was more appropriately a radial process, contracting to a focal point, and hence a linear process. Using cell area would have resulted in larger cells having disproportionately large fluctuations. Radial measures represent the average radius of a cell, irrespective of its shape anisotropy.

The trend in each cell radius was calculated using a boxcar average with a window of 5 minutes (red lines in Fig. 1B,C), and subtracted from raw cell radius to produce a detrended cell radius time series (see Fig. S1A,B in the supplementary material). The peaks and troughs in the detrended time series were identified where there was a change in gradient sign. We further removed peaks and troughs that were separated by very small amplitude radial changes (less than 0.13 μm). This threshold was set at a compromise level, maximising the removal of high-frequency noise while minimising the removal of genuine fluctuations. Using the remaining peak (π/2 radians) and trough (3π/2 radians) phase markers (colour-coded in Fig. S1A,B in the supplementary material) we calculated the amplitude (half the difference in radius between peak and trough) and cycle length (the duration of the cycle from peak to subsequent peak) of each cycle and the durations of the contraction and expansion parts to each cycle (see Fig. S1C,D in the supplementary material; Fig. 1D). Combinations of low amplitude and long cycle lengths were the signature of time periods when there were no discernible fluctuations, so we used cell radius fluctuation amplitude divided by cycle length as a measure of fluctuation strength, in μm per minute. Below a fluctuation strength threshold of 0.05 μm per minute (see Fig. S1C,D in the supplementary material, red bars; Fig. 1E, vertical dashed white line), cells were considered to have no discernible fluctuations and cycle length was registered as invalid.

For ubiECad-GFP and Sqh-mCherry double-labelled embryos, we classified and quantified fluctuations in average apical medial fluorescence intensities using the same methods as described above. We removed pixels at and within a distance of two pixels from the cell membranes from the analysis to exclude regions with fluorescence associated with the junctional pool. We used a threshold amplitude change of 1.3 greyscale for removing minor peaks and troughs.

Statistics

Throughout, 95% confidence intervals (Cumming et al., 2007) have been calculated and drawn in dashed lines on all relevant graphs or as error bars in figures. Non-overlapping confidence intervals indicate significant differences.

RESULTS

Quantitative analysis of AS cell shape fluctuations

During DC, AS cells exhibited periodic apical shape fluctuations in the plane of the zonula adherens (see Movie 1 in the supplementary material). We calculated the amplitude, cycle length and phase of cell radius fluctuations for all time points of all cells (see Materials and methods, Fig. 1A-C and Fig. S1 in the supplementary material). A time series analysis revealed consistent differences in the amplitude and cycle length of fluctuations as DC progressed, patterns that were repeated across multiple embryos (Fig. 1D-F). We observed three different modes of AS cell fluctuation, which can be correlated with three developmental epochs: early, slow and fast phases of DC. The early phase lasts ~45 minutes from the end of germ-band retraction to the start of DC and the beginning of the slow phase [time zero, defined as the onset of net AS contraction (Gorfinkiel et al., 2009)]. The fast phase starts 80 minutes later when the net AS contraction rate accelerates dramatically. In the early phase, AS cells fluctuated with large amplitudes (8-10% of cell radius) and long cycle lengths (4-minute cycles). At the onset of the slow phase, the amplitude decreased (6-7% of cell radius) and cycle length decreased (3-minute cycles). This change in cycle length at zero minutes was abrupt in all cells of the AS (Fig. 1F). By contrast, the decrease in proportional amplitude was slightly delayed relative to this transition (Fig. 1D). Finally, during the fast phase, only some cells displayed measurable fluctuations, and these were of low amplitude and short cycle length. The spatial and temporal pattern of decrease in both the amplitude and cycle length of fluctuations as DC progressed correlates with an increasing rate of contraction of AS cells as a whole (Gorfinkiel et al., 2009). More specifically, patterns of cycle length were mimicked by those of the rate of change in the trends in cell radius (Fig. 1G) and there was a strong linear relationship between the change in cell radius trends and cycle length (Fig. 1H). Although, overall, cell radius was correlated with cycle length, the detailed pattern of cycle lengths did not match that

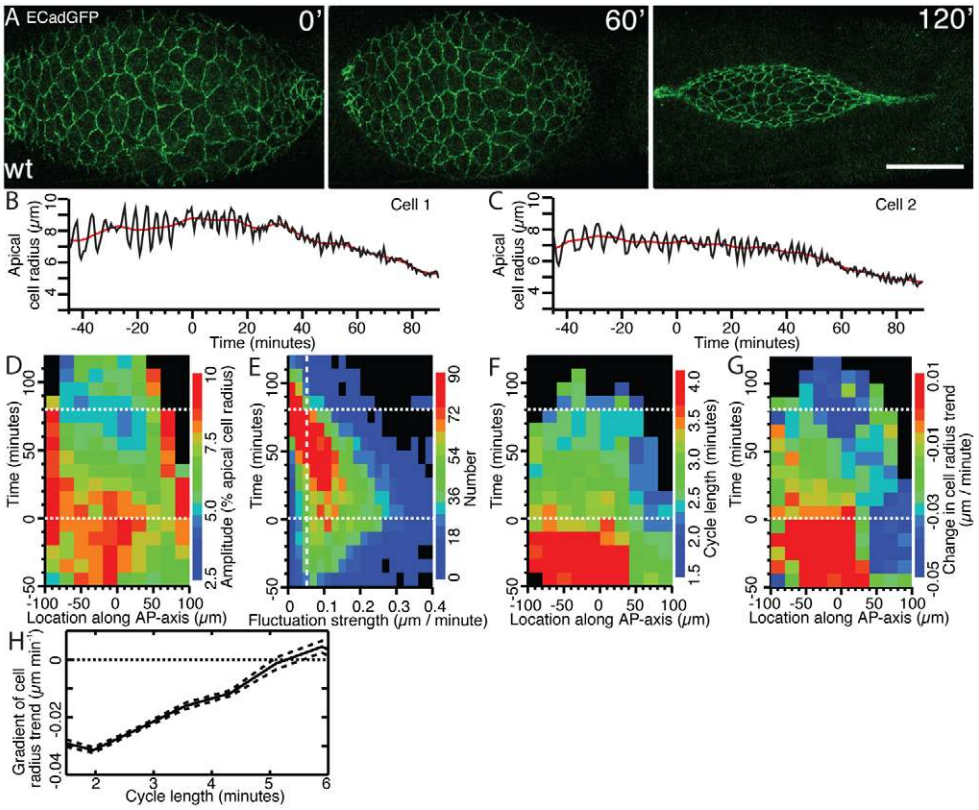

Fig. 1. Shape fluctuations of amnioserosa cells. (**A**) Still images from a time-lapse movie of a wild-type *Drosophila* embryo carrying the ubiECad-GFP transgene at 0, 60 and 120 minutes after the onset of amnioserosa (AS) contraction. Anterior is to the left in all images. (**B**,**C**) Time series of raw apical cell radius over time for two example cells (black line), also showing boxcar smoothed trends (red lines). (**D-H**) Analysis of cell radius fluctuations in data pooled from five wild-type embryos (average cells per embryo, 71.7; average minutes per cell, 115.8, sampled every 30 seconds). Horizontal dotted lines in D-G represent the transitions between early, slow and fast phases of DC. (D) Average fluctuation amplitude of AS cells as a function of their anterior-posterior (AP) location over time. Anterior is to the left in all similar panels. Legend bars to the right of each panel show colour values. (E) Histogram of fluctuation strength (amplitude/cycle length) over time. *y*-axis indicates the number of whole cycles (total number of cycles, 8209). Vertical dashed line represents the threshold value below which cells were classified as not fluctuating. (F) Average cycle length of AS cells as a function of their AP location over time (total number of valid cycles, 6196). (G) Trend in the change in cell radius of AS cells as a function of their AP location over time. (H) Trend in the change in cell radius as a function of fluctuation cycle length (dashed lines are ±95% confidence intervals).

of cell radius, and cells of the same area could exhibit very different fluctuating behaviour (Fig. 1D,F and see Fig. S2A in the supplementary material). Thus, of the various measures of fluctuating AS cells, fluctuation frequency and the rate of contraction were most intimately related.

Spatiotemporal organisation of contraction and expansion half cycles

To better understand the mechanics of cell fluctuations, we investigated how they were organised in time and across the tissue. We compared the duration of the contraction and expansion phases (half cycles) for each fluctuation cycle. The duration of contraction was shorter than that of expansion throughout DC, significantly so for early and slow phases of DC (Fig. 2A), suggesting that cell fluctuations might be driven by a robust cell-autonomous contractile phase. To investigate the organisation of fluctuations in space, we first broke the measures of cell radius fluctuation down into an elliptical description of the change in shape of each cell. We calculated the average invariant strain rates (Blanchard et al., 2009) for both the contraction and expansion phases of each cell fluctuation cycle (an example snapshot is shown in Fig. 2B), having first removed trends in cell shape strain rates. Major (longer) and minor (shorter) perpendicular strain rates describe the elliptical deformation rates of each cell. Contraction and expansion were both often anisotropic, with the major strain rate accounting for much of the change in shape of each cell. We therefore quantified the frequency of different combinations of strain rate pairs for each half cycle, and found that there was a significant positive relationship (Fig. 2C). However, the regression gradient was shallow (0.154), indicating that the majority of fluctuations in cell shape were indeed anisotropic. We then asked of the anisotropic fluctuations (those with a correlation ratio below 0.5, Fig. 2C) whether the orientation of contraction was followed by expansion in the same orientation, and vice versa, by calculating the change in orientation angle (Fig. 2D). The orientations of subsequent half cycle deformations were very similar, with 70% of orientation difference angles being less than 30 degrees. Orientations were significantly more similar for the transition from contraction to expansion than for the reverse (contraction to expansion n=4345; expansion to contraction n=4196, D=0.0736, P<<0.001; Kolmogorov-Smirnov two-sample test). That expansion is more likely to return an apical cell shape to its previous

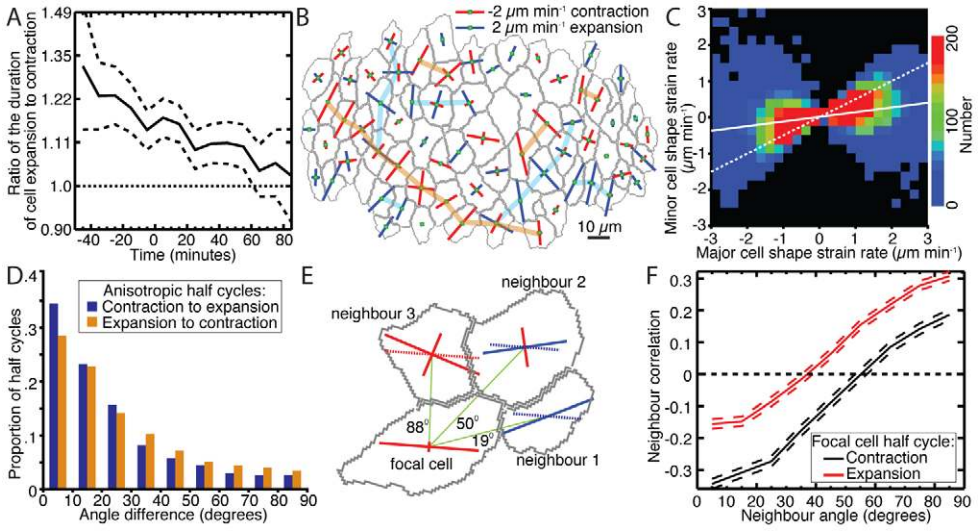

Fig. 2. Analysis of fluctuation half cycles. (**A**) Average ratio of the duration of expansion (trough to next peak) and contraction (peak to trough) half cycles for each valid fluctuation cycle over time (±95% confidence intervals; total number of valid cycles, 6196). (**B**) Snapshot from the start of the slow phase of DC showing how rapidly, and in what orientations, each cell was changing shape during its current half cycle. Tracked apical membrane shapes are shown in grey and cell shape strain rates are displayed as two perpendicular lines showing the rate of deformation (line length in μm per minute) in those orientations. The longer strain rate of each pair is the major strain rate (red indicates contraction, blue expansion). Orange and cyan ribbons show strings of cells with parallel contraction and expansion phases, respectively. Cells without drawn strain rates were not fluctuating. (**C**) Histogram of the minor versus major strain rate for each half cycle of each cell. The left-hand side of the graph, with negative major strain rates, represents the distribution of contracting half cycles, whereas the right-hand side of the graph represents expansion (5655 contraction and 5744 expansion half cycles from five wild-type *Drosophila* embryos have been pooled). Solid white line indicates regression gradient (0.154 with a standard error of 0.0039). Data less correlated than 0.5 (dotted white line) were considered anisotropic, with a dominant orientation of deformation. (**D**) The orientation of the major strain rate for each anisotropic half cycle was compared with the orientation of the major strain rate of the next half cycle for each cell. The difference in orientation angle for the transition from contraction to expansion and vice versa have been plotted separately (the number of half cycle pairs was 4196 and 4345, respectively, pooled from five embryos). (**E**) Focal cell and three example neighbours, showing average half cycle strain rates (solid red and blue lines). Neighbour strain rates projected onto the same orientation as the major strain rate of the focal cell are shown in dotted red or blue lines. The correlation ratio between the length of these projected strain rates for each neighbour (*a*) and of the major strain rate of each focal cell (*b*) was calculated as *a*/*b*. Neighbours were also classified by their angle to the orientation of the major strain rate of the focal cell (green lines, angles in degrees shown). (**F**) Correlation ratio between the major strain rates of all cells and those of all their neighbours versus the angle of the neighbour, as calculated in E (data pooled from five embryos; number of neighbour pairs was 22577 and 22354 for contracting and expanding half cycles, respectively). Dashed lines indicate ±95% confidence intervals.

expanded shape than vice versa suggests that the equilibrium shape of a cell apex is closer to its expanded shape, and that active contraction drives cell apices away from this equilibrium.

These observations raised interesting questions about how cells accommodate the half cycle fluctuations of their neighbours. To assess this, we investigated the correlation ratio of the major strain rate of each cell with the strain rate in the same orientation of all of its neighbours, calculated as a function of the angle of the neighbouring cell (Fig. 2E). In this example, neighbour 1 is nearly in line with the major orientation of contraction of the focal cell and is expanding in that orientation and so is strongly anti-correlated. Neighbour 3 is in a perpendicular position, with a contraction that is strongly correlated with the focal cell. Neighbours in line with the orientation of contraction had anti-correlated strain rates (–0.35; Fig. 2F, black line). This means that about one-third of the contraction of a cell is accommodated by cells beyond its immediate neighbours. The strain rates of neighbours perpendicular to the major strain rate of the focal cell were positively correlated (0.2), suggesting that cell fluctuations are coordinated in rows. These patterns can be seen in Fig. 2B (orange ribbons), in which some cells with parallel anisotropic strain rates are arranged in rows. For expansion half cycles, neighbours in line with the orientation of expansion of the focal cell had strain rates that were again anti-correlated (–0.15), but significantly less so than for contracting half cycles. This means that about two-thirds of cell expansion is accommodated by cells beyond its immediate neighbours. Neighbours perpendicular to the orientation of expansion had strain rates that were significantly more strongly correlated (0.31; Fig. 2F, red line). Rows of expanding anisotropic neighbours can also be seen in Fig. 2B (cyan ribbons). These differences again suggest that contraction is the more active process, having the most dramatic effect on immediate neighbours in line with the orientation of contraction. Expansion is better organised into rows of cells that expand in parallel, often accommodating contraction at a distance beyond immediate neighbours.

The role of the cytoskeleton in cell shape fluctuations

Fluctuating behaviour similar in scale to that described here has been correlated with the activity of the actin-myosin cytoskeleton (Martin et al., 2009; Salbreux et al., 2007), and this led us to image actin and myosin dynamics in AS cells using fluorescent protein reporters. We observed that the actin-binding domain of Moesin fused to GFP (Moe-GFP), and the myosin regulatory light chain, Spaghetti squash (Sqh), fused to GFP or mCherry (Sqh-GFP or Sqh-mCherry) were present at the apices of cells in two distinct structures: as a dynamic

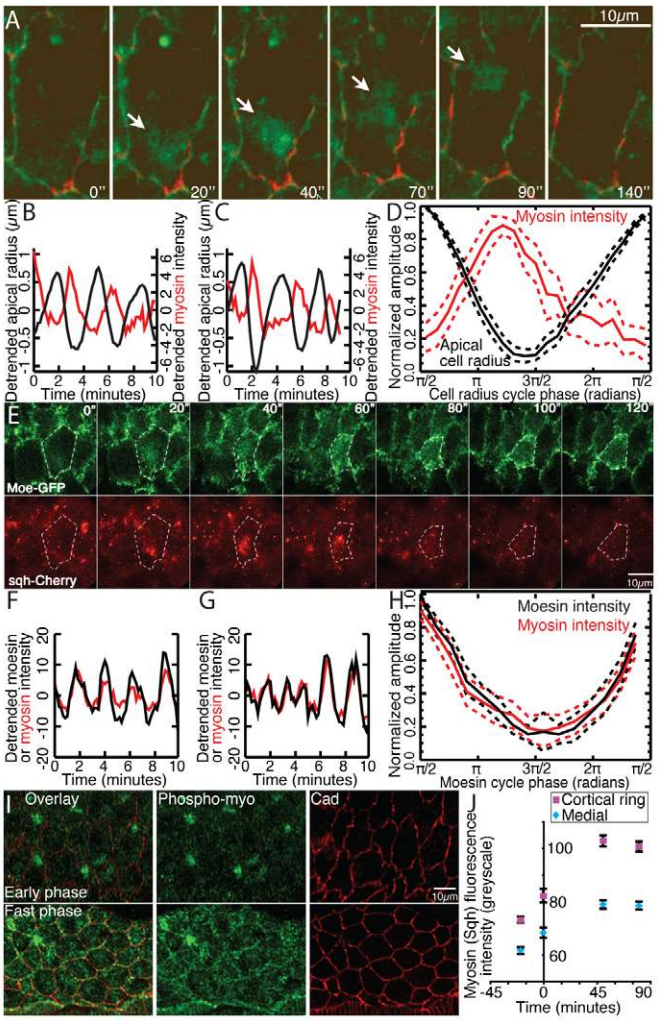

Fig. 3. Myosin and actin dynamics during amnioserosa cell shape fluctuations. (**A**) AS cell expressing Sqh-Cherry (green) and ubiECad-GFP (red), showing contraction (0-90 seconds) and expansion (90-140 seconds) during the early phase of DC. A Sqh focus starts at the bottom of the cell (20 seconds) and flows up to the top of the cell by 90 seconds (arrows) as the cell contracts. The cell then expands, with low myosin fluorescence levels (140 seconds). (**B**,**C**) Ten-minute time series for two example cells sampled every 10 seconds, showing fluctuations in cell radius (black line) and medial Sqh fluorescence intensity (red line) during the early phase of DC. Time series have been detrended to remove trends in net apical contraction and bleaching decay, respectively. (**D**) Average shape of normalised cell radius (black line, ±95% confidence intervals) and medial Sqh fluorescence (red line, ±95% confidence intervals) cycles for equivalent cells and time points during the early phase of DC (data pooled from four embryos; total cell minutes, 167; sampled every 10 seconds). Note that cell radius contraction correlates with increase in Sqh fluorescence, but fluorescence reduction precedes cell expansion. (**E**) Still images covering 2 minutes from a time-lapse movie of an embryo carrying the Moe-GFP (green) and Sqh-mCherry (red) encoding transgenes showing contraction and some expansion for the central cell (dotted outline). (**F**,**G**) Ten-minute time series for two cells during the early phase of DC, showing Moe (black line) and Sqh (red line) fluorescence intensities in a central medial disc. (**H**) Average shapes of normalised cycles of Moe and Sqh fluorescence intensities (±95% confidence intervals; total cell minutes, 86; sampled every 10 seconds) for equivalent cells and time points during the early phase of DC. (**I**) Stage 13 (early DC, top row) and stage 15 (fast phase, bottom row) embryos stained for phospho-Myosin light chain 2 (green) and E-Cadherin (red). (**J**) Average unbleached Sqh-mCherry fluorescence intensity of junctional and medial apical regions at different stages of DC (data pooled from four, four, two and one embryo starting at –20, 0, 50 and 80 minutes from the onset of AS contraction, respectively; average number of cells per embryo, 19.3). Shown ±95% confidence intervals; non-overlapping confidence intervals indicate significantly different means.

apical medial network, and in a cortical ring at cell-cell adherens junctions. During the early and slow phases of DC, we observed accumulations, or foci, of Moe-GFP and Sqh-GFP that appeared transiently and often moved as a wave across the apical surface of cells (see Movies 2 and 3 in the supplementary material). Foci coalesced and disappeared both at the centre of the apical cortex and near the lateral membranes.

The formation of Moe-GFP and Sqh-GFP foci coincided with local displacements of the membrane towards the foci, suggesting that they might be contributing to the cell shape fluctuations (Fig. 3A). We used double-labelled Sqh-mCherry and E-Cadherin-GFP (ECad-GFP) embryos (see Movie 5 in the supplementary material) to quantify simultaneously the intensity of the apical medial myosin (excluding the junctional myosin) and changes in the apical cell radius. Average apical medial myosin fluorescence intensity was inversely correlated with cell radius (Fig. 3B-D). The rapid increase in myosin fluorescence intensity reached a peak that preceded the trough of cell radius (Fig. 3D), reflecting the subcellular nature of the fluctuating behaviour, in which expansion at one end of a cell can occur simultaneously with contraction at the other end, and where the greatest extent of myosin fluorescence occurred mid-wave (Fig. 3A).

Simultaneous imaging of Moe-GFP and Sqh-mCherry (see Movie 6 in the supplementary material) revealed that both proteins co-localised in time and space at these dynamic foci (Fig. 3E), although Sqh-mCherry localisation was sharper than the more diffuse Moe-GFP. We quantified simultaneously the intensity of Moe-GFP and Sqh-mCherry fluorescence at a subcellular scale. The average fluorescence intensity over time within a circle at the centre of each cell (diameter 4.2 μm) was measured (Fig. 3F,G). Peaks in fluorescence were identical for Moe-GFP and Sqh-mCherry, and although myosin fluorescence was lost slightly before actin, these differences were not significant (Fig. 3H). Interestingly, fluorescence gain was faster than fluorescence loss, suggesting differences in the mechanism of foci assembly and disassembly. In contrast to these similarities at cell centres, we sometimes observed an increase in the localisation of Moe-GFP, but not of Sqh-mCherry, at the cell edges.

Altogether, these observations suggest that cell radius fluctuations are driven by active apical actin-myosin contraction. The increase in Moe-GFP and Sqh-mCherry fluorescence at a contractile focus [peaks were frequently double the trough values in non-detrended (see Materials and methods) data] was much greater than would have been expected simply from an increase in the density of existing myosin fluorescence due to cell contraction (maximum 20%; see Fig. S1C,D in the supplementary material). Combined with the divorce between myosin peak and area trough, and the similarity of the Moe and Sqh patterns and dynamics, these results suggest that large-scale actin-myosin structures were being assembled and disassembled in each cell contraction cycle.

To better understand the role of the apical medial network of myosin in the apical contraction of AS cells, we analysed its behaviour as DC progressed. We quantified the average apical medial myosin at the start of short movies covering the early, slow and fast phases of DC and found that fluorescence levels of apical medial myosin increased significantly over time (Fig. 3J). Furthermore, apical medial myosin progressively occupied the whole apical surface of AS cells and eventually formed a continuous sheet spanning the whole tissue (see Movie 4 in the supplementary material). These changes in the localisation of myosin were also evident in fixed embryos stained with an anti-phospho-myosin antibody (Fig. 3I). During the early and slow phases of DC, phospho-myosin accumulated in foci at the apical surface of AS cells, similar to the Sqh-mCherry foci observed in live embryos. During the fast phase of DC, there was a continuous labelling of phospho-myosin at the apical surface of AS cells (Fig. 3I). Thus, during DC there is the progressive formation of an apical actin-myosin meshwork that starts as discrete and dynamic foci moving along the apical cell surfaces and gradually forms a continuous, although still dynamic, network.

Together with the increase in apical medial myosin, we observed that the average levels of junctional myosin also increased as DC progressed (see Movie 3 in the supplementary material; Fig. 3J). Immunostaining with an anti-phospho-myosin antibody also showed a moderate increase in the levels of phospho-myosin at cell-cell junctions (Fig. 3I). The change in shape of AS cellular membranes during DC from wiggly to straight interfaces (Fig. 3I) is indicative of an increase in cortical tension (Lecuit and Lenne, 2007) and is thus in agreement with the observed increase in the levels of junctional myosin.

Altogether, our results suggest that actin-myosin activities, both at the apical surface of AS cells and at the level of cell-cell junctions, are responsible for the apical contraction of these cells. In support of this, laser-ablation experiments in AS cells have shown the presence of tensile stress at both cell-cell interfaces and cell centres (Ma et al., 2009).

Perturbing cytoskeletal dynamics changes the pattern of cell shape fluctuations

In order to test whether there was an underlying causality to the correlation between actin-myosin activity and the macroscopic cell shape fluctuations, we modified cytoskeletal dynamics exclusively in the AS cells using the UAS-Gal4 system. The overactivation of myosin through the ectopic expression of a constitutively active myosin light chain kinase (ctMLCK) has been shown to induce the premature contraction of AS cells (Homem and Peifer, 2008). Live imaging of ASGal4/UAS-ctMLCK embryos confirmed that there was a premature contraction of the whole tissue, evident in the elongated shape of the AS in the anteroposterior axis soon after germ-band retraction (see Movie 7 in the supplementary material and Fig. 4A). This shape at such an early stage is evidence that contraction of the AS is enhanced and dominates over zippering (Hutson et al., 2003). ASGal4/UAS-ctMLCK cells exhibited fewer shape fluctuations than the wild type and their mean amplitude remained remarkably constant over time and space (Fig. 4B). Cycle lengths also appeared relatively constant over time, at 3-3.5 minutes on average (Fig. 4C,D). However, cell shapes were unusual, with smaller cell apices (see Fig. S2B in the supplementary material), more isotropic shapes (see Fig. S3 in the supplementary material) and straighter apicolateral membranes (Fig. 4A) than wild-type cells of the same stage. Importantly, in these embryos, AS cells produced frequent apical blebs (see Fig. S4A,B in the supplementary material) (Charras et al., 2006; Paluch et al., 2006).

To alter the actin network in a different manner, we used an activated form of Diaphanous (Dia^{CA}), an actin regulator that promotes filament elongation. As reported previously, the ectopic expression of Dia^{CA} induces a premature contraction of the AS (Homem and Peifer, 2008). Live imaging of ASGal4/UAS-Dia^{CA} embryos (see Movie 8 in the supplementary material; Fig. 4E) showed that AS cells exhibit negligible cell area fluctuations (Fig. 4F). Cell apices appeared small (see Fig. S2C in the supplementary material) and significantly more isotropic than in the wild type (see Fig. S3 in the supplementary material), as was the case for the ectopic expression of ctMLCK. Cell membranes were noticeably more wiggly than in the wild type (compare Fig. 4E with Fig. 1A).

To understand how these changes in the cell area fluctuations of AS cells correlated with cytoskeletal dynamics, we simultaneously imaged AS cells with ECad-GFP and Sqh-mCherry under these two perturbed conditions (see Movies 9 and 10 in the supplementary material). In ASGal4/UAS-ctMLCK embryos, most AS cells still showed dynamic foci of myosin accumulation, but with a different signature from the wild type. Apical myosin fluorescence intensity was again inversely correlated with apical cell radius, but the peak of myosin was now coincident with the trough of cell radius (Fig. 4G,H). We think that bleb contraction results in a knot of high myosin concentration that persists after bleb contraction is complete (for example, see Fig. S4B in the supplementary material, red arrow) (Charras et al., 2006; Paluch et al., 2006). By contrast, in AS cells from ASGal4/UAS-Dia^{CA} embryos, we rarely observed foci of myosin accumulation. Neither apical myosin fluorescence nor cell shape fluctuated (Fig. 4I).

Immunostaining of mutant embryos with an anti-phospho-myosin antibody showed changes in the levels and the subcellular localisation of phospho-myosin in AS cells compared with equivalent stages in the wild type. Similar observations have been reported in the embryonic epidermis (Bertet et al., 2009; Fernandez-Gonzalez et al., 2009). In ASGal4/UAS-ctMLCK embryos, there was a clear increase in phospho-myosin levels at cell-cell junctions, in a disrupted apical medial population (Fig. 4J) as well as sub-apically. Total apical myosin was significantly greater than in wild-type embryos during both early (wild type, n=5; ctMLCK, n=3; t=8.16, P<0.001; t-test) and fast (wild type, n=6; ctMLCK, n=3; t=2.68, P=0.0365; t-test) phases. By contrast, in ASGal4/UAS-Dia^{CA} embryos there was no discernible increase in junctional or apical medial myosin (Fig. 4K). However, by the fast phase, we observed a relative increase in sub-apical myosin levels. Compared with wild-type fast-phase embryos, in which there was greater total apical than sub-apical myosin, in ASGal4/UAS-Dia^{CA} embryos the reverse was true (Fig. 4L) and this difference was significant (wild type, n=5; ASGal4/UAS-Dia^{CA}, n=4; t=4.45, P<0.003; t-test). This suggests that whereas in ASGal4/UAS-ctMLCK embryos there was an increase in tension throughout AS cells, in ASGal4/UAS-Dia^{CA} there was no increase in junctional tension but an increase in tension in the sub-apical and lateral cortex. These observations could explain the differences in the shape of the membranes in these two perturbed conditions, with straight membranes in the former and wiggly membranes in the latter.

To complement the above mutants with enhanced myosin or actin activity, we analysed the effect of reducing actin and myosin activity on the behaviour of AS cells. Both myosin phosphorylation

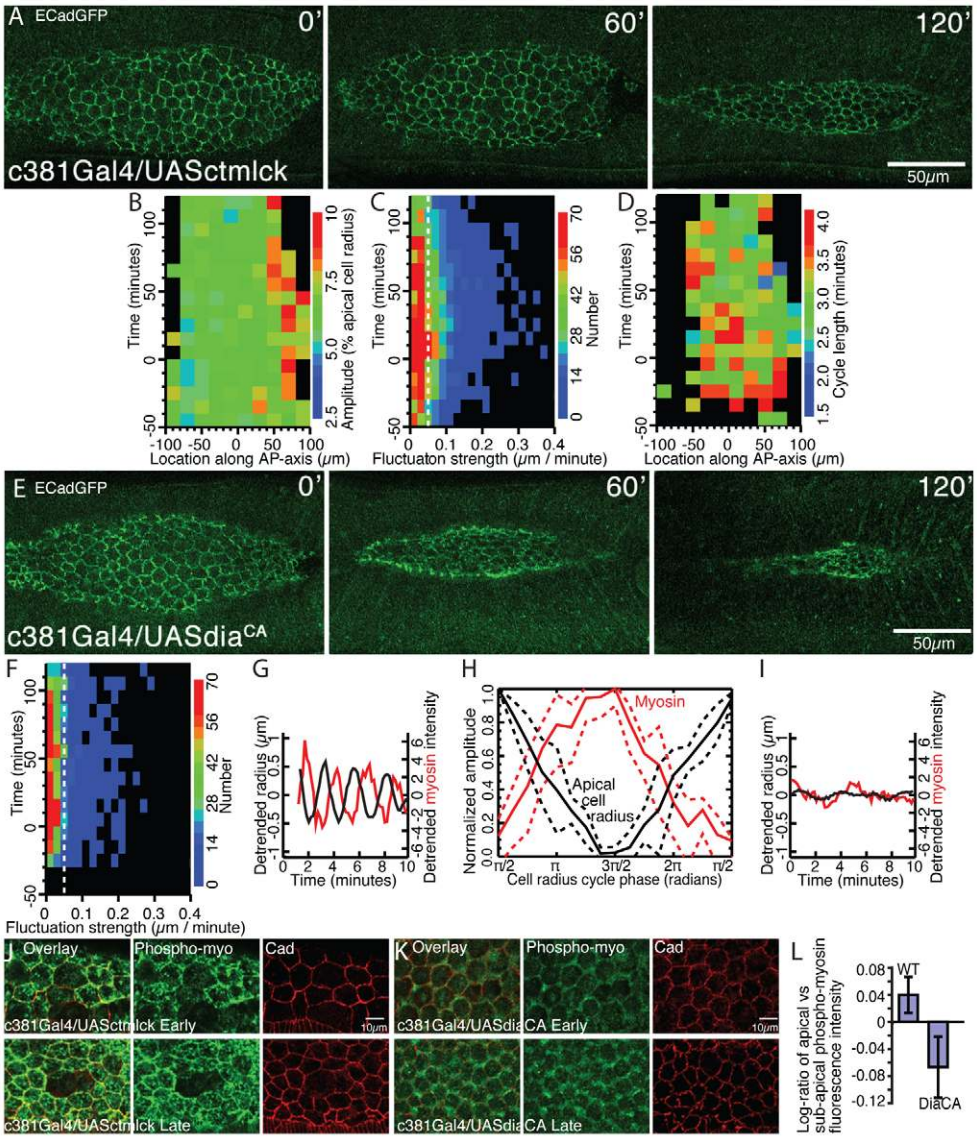

Fig. 4. Cell shape fluctuations and myosin dynamics in embryos with perturbed myosin and actin activity. (**A-D**) Analysis of AS cell fluctuations of ASGal4/UAS-ctMLCK *Drosophila* embryos. (A) Still images from a time-lapse movie of an example ASGal4/UAS-ctMLCK; ubiECad-GFP embryo at 0, 60 and 120 minutes after the onset of AS contraction (staging of perturbed embryos was according to the end of germ-band retraction and the morphogenesis of the posterior spiracles). (B-D) Analysis of cell radius fluctuations as described for Fig. 1D-F. Data were pooled from three embryos (average cells per embryo, 79.3; average minutes per cell, 147.5; sampled every 30 seconds). (B) Average fluctuation amplitude. (C) Histogram of fluctuation strength (total number of cycles, 4022). (D) Average cycle length (number of valid cycles, 1524). (**E**,**F**) Analysis of AS cell fluctuations of ASGal4/UAS-Dia^{CA} embryos. (E) Still images from a time-lapse movie of an example ASGal4/UAS-Dia^{CA}; ubiECad-GFP embryo at 0, 60 and 120 minutes after the onset of AS contraction. (F) Analysis of cell radius fluctuations as described for Fig. 1E, here for ASGal4/UAS-Dia^{CA} embryos. Data pooled from four embryos [average cells per embryo, 58.2; average minutes per cell, 93.6; sampled every 30 seconds; total number of cycles (F), 2188]. Note that there were very few cycle length data for these embryos because the fluctuation strength was almost always below threshold (F). (**G**) Ten-minute time series of an example cell from an ASGal4/UAS-ctMLCK embryo, sampled every 10 seconds, showing fluctuations in cell radius (black line) and medial Sqh-mCherry fluorescence intensity (red line). (**H**) Average shape of normalised cell radius (black line, ±95% confidence intervals) and medial Sqh fluorescence (red line, ±95% confidence intervals) cycles for equivalent cells and time points (total number of cycles, 89) shortly after germ-band retraction. (**I**) Ten-minute time series for an example cell from an ASGal4/UAS-Dia^{CA} embryo, sampled every 10 seconds, showing cell radius (black line) and medial Sqh fluorescence intensity (red line). No fluctuations were detected. (**J**,**K**) ASGal4/UAS-ctMLCK (J) and ASGal4/UAS-Dia^{CA} (K) embryos stained for phospho-Myosin light chain 2 (green) and E-Cadherin (red) shortly after germ-band retraction (top row) and during the fast phase of DC (bottom row). (**L**) Comparison of the fluorescence intensities of total apical and sub-apical phospho-myosin in wild-type and ASGal4/UAS-Dia^{CA} embryos. Error bars indicate s.d.

mediated by Rho kinase and actin polymerisation mediated by Dia are major effectors of the small GTPase RhoA (Rho1 – FlyBase) (Bishop and Hall, 2000; Wheeler and Ridley, 2004). AS cells expressing a dominant-negative form of RhoA did not fluctuate, nor did they consistently reduce their apical surface area, and as development progressed the tissue tore apart (see Movie 10 and Fig. S5A in the supplementary material). They did not form Sqh-mCherry foci, nor was there localisation at cell-cell junctions (see

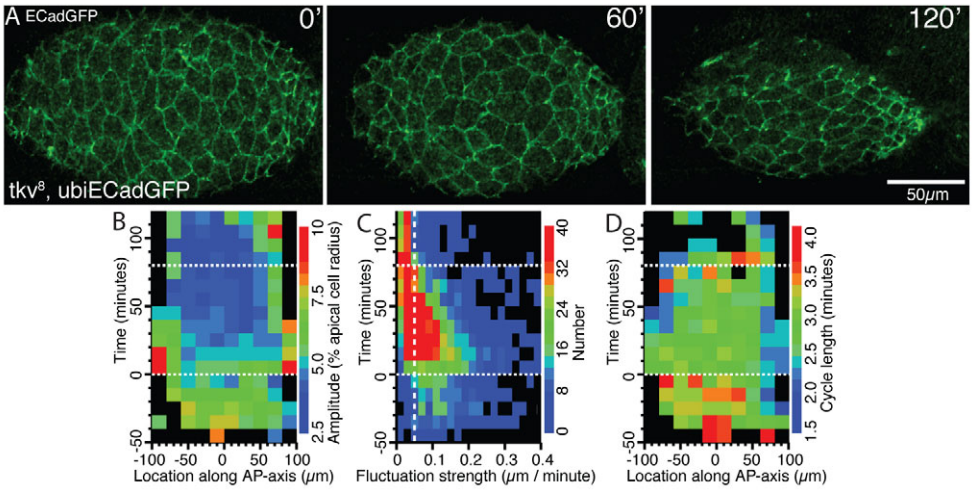

Fig. 5. Cell shape fluctuations in *tkv* mutants. (**A**) Still images from a time-lapse movie of a *tkv*; ubiECad-GFP zygotic mutant *Drosophila* embryo at 0, 60 and 120 minutes after the onset of AS contraction. (**B-D**) Analyses as described for Fig. 1D-F. Data were pooled from four embryos (average cells per embryo, 36.2; average minutes per cell, 123.3; sampled every 30 seconds). (B) Average fluctuation amplitude. (C) Histogram of the strength of fluctuation (total number of cycles, 2720). (D) Average cycle length (total number of valid cycles, 1785).

Fig. S5B in the supplementary material). Residual movements of AS cells seemed to be a passive consequence of other morphogenetic movements occurring in the embryo.

Altogether, these results show that the presence and signature of cell fluctuations and the shape of cellular membranes depend on the relative strengths, dynamics and localisation of cellular actin-myosin. We suggest that the progressive accumulation of myosin as DC proceeds increases cell contractility.

Dpp and AS cell fluctuations

The results presented above raise the important question of what causes the changes in actin-myosin localisation over time, leading to an increase in cell contractility. One possibility is that these changes are the result of an autonomous programme of AS cell contraction. Alternatively, signals from the epidermis could activate myosin and/or actin activities.

It has been proposed that the damping of AS cell fluctuations over time is a consequence of the assembly of the supracellular actin cable at the leading edge (LE), which would act in a ratchet-like mechanism (Solon et al., 2009). In this model, contraction of the cable would prevent the relaxation of AS cells after a contraction cycle. We tested this by asking how the amplitude and cycle length of fluctuations progress in a mutant in which the supracellular actin cable and zippering processes are defective. Dpp, a member of the BMP/TGFβ family of secreted signals, is expressed in the dorsal-most epidermal (DME) cells during stage 11, and also later on, during stage 13. Zygotic mutants for the Dpp receptor *thickveins* (*tkv*) exhibit defects in DC (Riesgo-Escovar and Hafen, 1997); specifically, DME cells have defects in dorsoventral elongation, the LE does not maintain an actin-myosin cable and zippering movements are absent (García Fernández et al., 2007) (Ricos et al., 1999). The proposal for the role of the actin-myosin cable suggests that these embryos should not show a damping of fluctuations.

Live imaging (see Movie 11 in the supplementary material) revealed that in these mutants, AS cells exhibited a spatial and temporal pattern of shape fluctuations that shared strong similarities with that of the wild type (Fig. 5A-D). Importantly, AS cells displayed a decrease in the amplitude and cycle length of fluctuations as they transited from the early to the slow phase of DC. AS cells exhibited a wild-type evolution in cell shape, from anisotropic during the early phase to a more isotropic shape during the slow and fast phases (see Fig. S3 in the supplementary material), indicative of an increase in apical tension. Eventually, AS cells in *tkv* mutants contracted completely. In spite of these similarities, fluctuation amplitude and cycle length during the early phase were lower in *tkv* mutants than in wild-type embryos (Fig. 5B,D).

Thus, the damping of cell shape fluctuations, the changes in cell shape that are a signature of increased apical tension, and the eventual contraction of AS cells still occur in *tkv* mutants, even though these embryos were able to maintain neither an actin cable at the LE nor epidermal cell elongation, and did not develop zippering movements. Although these results do not rule out the possibility that segments of actin cable remain functional in *tkv* mutants, nor that in wild-type embryos the epidermis, the actin cable and zippering movements contribute to the patterned contraction of AS cells, they suggest to us that AS cells have a robust intrinsic programme of contraction.

DISCUSSION

The molecular basis for cell fluctuations

The process of DC relies on the coordination of the elongation of epidermal cells and contraction of the AS. Throughout the early stages of this process the AS cells exhibit fluctuations of their apical area (Solon et al., 2009) (this work). We have shown that this fluctuating behaviour is driven by transient actin-myosin accumulations at the apical cortex of cells, involving the assembly, contraction and disassembly of large-scale actin and myosin structures. The formation and disassembly of foci could result from the self-organising properties of myosin and actin and the presence of specific regulators, which are known to spontaneously form active networks, asters and rings in vitro (Backouche et al., 2006; Haviv et al., 2006). Tension generated by the contraction of neighbouring cells (Solon et al., 2009) (this work), the sudden loss of tension due to detachment of actin from the cell membrane, spontaneous catastrophic collapse (Howard, 2009), and the

stretching of the apical membrane resulting in the influx of ions such as calcium (Salbreux et al., 2007), could all contribute to the timing and location of fluctuations.

Junctional and medial actin-myosin populations

Differences in the absolute and relative strengths of actin-myosin structures in distinct subcellular populations provide an explanation for the patterns that we have observed in wild-type and mutant embryos. Our observations show that throughout DC the amounts of myosin increase in two subcellular populations: in a cortical ring and in a medial apical network. The amount of myosin at cell-cell junctions determines the shape of cell membranes: low levels lead to wiggly membranes and increasing levels of junctional myosin lead to the straightening of the membranes. The amount of actin-myosin in the medial population determines the fluctuating behaviour of cells: low levels lead to low-frequency fluctuations and no tissue contraction, as seen in the early phase of DC; intermediate levels lead to high-frequency fluctuations and slow tissue contraction, as seen in the slow phase of DC; and high levels lead to a coherent, but dynamic, sheet of actin-myosin across cells that was strongly contractile, as seen in the wild-type fast phase.

Increasing the amounts of both junctional and medial myosin in ASGal4/UAS-ctMLCK embryos led to premature apical contraction, precocious straight cell membranes and isotropic cell shapes, which are a signature of high cortical tension (Lecuit and Lenne, 2007). By contrast, in ASGal4/UAS-Dia^{CA} embryos, low junctional myosin levels throughout DC gave rise to wiggly apical membranes. However, these cells showed precocious apical contraction and no discernible apical shape fluctuations. We observed an increase in myosin levels at a sub-apical position, which suggests to us that in these cells contraction is not only apical but spans the sub-apical and lateral axis. This sub-apical and lateral contraction of AS cells could be an impediment to apical shape fluctuations, as apical contraction must be accommodated by basal or lateral expansion.

Overactivating myosin led to apical blebbing in AS cells. Blebbing results from an increase in the ratio of cortical tension to cortex-membrane adhesion (Charras and Paluch, 2008) and is associated with transient actin-myosin accumulations similar to those observed here (Charras et al., 2008). We looked for, but could find no evidence of, blebs in AS cells in wild-type embryos. We suggest that dynamic actin-myosin structures are the more general property of cells, which in combination with high cortical tension or weak cortex-membrane adhesion can lead to blebs.

The supracellular organisation of fluctuations

Previous results have shown that neighbours oscillate mainly in anti-phase (Solon et al., 2009). Our results reveal a more subtle picture, with anti-phase correlation predominantly in one orientation and in-phase correlation perpendicular to this. This combination results in interesting patterns, with rows or patches of cells that become synchronised for short periods of time and represent an emergent property of the system. We expect that some sort of multicellular pattern is inevitable because of the requirement to maintain a coherent epithelium while cells fluctuate. However, the patterns also suggest that cell fluctuations can become entrained locally and for short periods. Our analysis of the dynamics of cell shape suggests that cell contraction is the active process, but that fluctuating behaviour of a cell can be influenced and the timing of active contraction altered by the forces generated by immediate neighbours and more distant cells. Thus, the organisation of apical contractions and expansions at the multicellular scale arises from the feedback in both directions between intrinsic cell behaviour and mechanical context.

Amnioserosa contraction

We wanted to understand how changes in actin-myosin behaviour at a subcellular scale resulted in the patterned contraction of the AS. There is a gradual increase in the rate of contraction of individual cells that strongly accelerates with the onset of zippering behaviour (Gorfinkiel et al., 2009). These changes were correlated primarily with a shortening of fluctuation cycle length. Our results suggest that these changes result from an increase in both apical medial and junctional myosin levels. The overall increase in myosin levels and the formation of a continuous actin-myosin network could provide the molecular basis for the transition of the AS to a more solid tissue (Ma et al., 2009).

What causes the increase in apical myosin levels? One possibility is that it is induced by a chemical or mechanical signal from the epidermis. A radial gradient of fluctuations (Solon et al., 2009) and of the rate of contraction of AS cells (Gorfinkiel et al., 2009) suggests that the epidermis is providing some information for the patterned contraction of the AS. However, the analysis of *tkv* mutants shows that even when the mechanical properties of DME cells have been altered and Dpp signalling is compromised (B. García Fernández, PhD thesis, New University of Lisbon, 2007) (Ricos et al., 1999), AS cells change their fluctuation behaviour in a similar pattern to the wild type and finally contract. This reveals that several processes that are individually redundant ensure DC. DC could result from an AS-autonomous programme of increasing medial and junctional myosin (and/or actin), through changes in the dynamics of actin and myosin activity, of intracellular trafficking or of cell adhesion. Alternatively, apical myosin might increase as a result of the fluctuating behaviour of AS cells and the build-up of tension due to neighbour contractions. Whatever the mechanism, it is likely that an increase in myosin activity involves activation of the Rho GTPase, which has a central role both in integrating mechanical and structural cues and in regulating myosin-based tension (Ingber, 2008) (this work).

The function of cell fluctuations in dorsal closure

AS cells fluctuate at low frequencies for a long period during early DC without any tissue contraction. High-frequency fluctuations drive moderate cell and tissue contraction during the slow phase, before they disappear in the transition to rapid tissue contraction. This raises the question of whether fluctuations have a function, as it is at least theoretically possible that contraction could be achieved in a smooth manner. One can speculate that cell fluctuations would be a way to maintain a basic level of cell activity that could be turned easily into morphogenetically relevant behaviours (Farhadifar et al., 2007; Rauzi et al., 2008). Cell fluctuations could, more simply, be an epiphenomenon of the self-organised dynamics of actin and myosin. Alternatively, pulsatile contraction might ensure that differences in apical tension are equilibrated between neighbouring cells, ensuring coordination in the contraction of cells across the tissue. Our analysis of neighbour relations suggests that fluctuations allow for a certain degree of coordination between cells. A combination of empirical investigation and modelling will be crucial to understand the importance of fluctuations per se during morphogenesis.

Note added in proof

Recent work shows that the formation of transient actomyosin networks correlates with the apical constriction of AS cells (David et al., 2010). The results are compatible with the frequency data measured in our study.

Acknowledgements
We thank Stephen Young, Pietro Cicuta, Alexandre Kabla, Joaquín de Navascués, Benedicte Sanson, Carlos Torroja and members of our labs for useful discussions; and D. Kiehart, A. Martin, J. Zallen, P. Rorth, M. VanBerkum, B. García Fernández, C. Klämbt and T. Lecuit for stocks. We are very grateful to Pablo Barrecheguren and Joaquín de Navascués for their invaluable help during the resubmission of the manuscript. This work was supported by a Biotechnology and Biological Sciences Research Council grant to N.G. and A.M.-A. and an Engineering and Physical Sciences Research Council grant to R.J.A.

Competing interests statement
The authors declare no competing financial interests.

Supplementary material
Supplementary material for this article is available at
http://dev.biologists.org/lookup/suppl/doi:10.1242/dev.045872/-/DC1

References

Backouche, F., Haviv, L., Groswasser, D. and Bernheim-Groswasser, A. (2006). Active gels: dynamics of patterning and self-organization. *Phys. Biol.* **3**, 264-273.
Bertet, C., Rauzi, M. and Lecuit, T. (2009). Repression of Wasp by JAK/STAT signalling inhibits medial actomyosin network assembly and apical cell constriction in intercalating epithelial cells. *Development* **136**, 4199-4212.
Bishop, A. L. and Hall, A. (2000). Rho GTPases and their effector proteins. *Biochem. J.* **348**, 241-255.
Blanchard, G. B., Kabla, A. J., Schultz, N. L., Butler, L. C., Sanson, B., Gorfinkiel, N., Mahadevan, L. and Adams, R. J. (2009). Tissue tectonics: morphogenetic strain rates, cell shape change and intercalation. *Nat. Methods* **6**, 458-464.
Brand, A. H. and Perrimon, N. (1993). Targeted gene expression as a means of altering cell fates and generating dominant phenotypes. *Development* **118**, 401-415.
Charras, G. and Paluch, E. (2008). Blebs lead the way: how to migrate without lamellipodia. *Nat. Rev. Mol. Cell Biol.* **9**, 730-736.
Charras, G. T., Hu, C. K., Coughlin, M. and Mitchison, T. J. (2006). Reassembly of contractile actin cortex in cell blebs. *J. Cell Biol.* **175**, 477-490.
Charras, G. T., Coughlin, M., Mitchison, T. J. and Mahadevan, L. (2008). Life and times of a cellular bleb. *Biophys. J.* **94**, 1836-1853.
Cumming, G., Fidler, F. and Vaux, D. L. (2007). Error bars in experimental biology. *J. Cell Biol.* **177**, 7-11.
David, D. J. V., Tishknia, A. and Harris, T. J. C. (2010). The PAR complex regulates pulsed actomyosin contractions during amnioserosa apical constriction in *Drosophila*. *Development* **137**, 1645-1655.
Edwards, K. A., Demsky, M., Montague, R. A., Weymouth, N. and Kiehart, D. P. (1997). GFP-moesin illuminates actin cytoskeleton dynamics in living tissue and demonstrates cell shape changes during morphogenesis in Drosophila. *Dev. Biol.* **191**, 103-117.
Farhadifar, R., Roper, J. C., Aigouy, B., Eaton, S. and Julicher, F. (2007). The influence of cell mechanics, cell-cell interactions, and proliferation on epithelial packing. *Curr. Biol.* **17**, 2095-2104.
Fernandez-Gonzalez, R., Simoes Sde, M., Roper, J. C., Eaton, S. and Zallen, J. A. (2009). Myosin II dynamics are regulated by tension in intercalating cells. *Dev. Cell* **17**, 736-743.
Franke, J. D., Montague, R. A. and Kiehart, D. P. (2005). Nonmuscle myosin II generates forces that transmit tension and drive contraction in multiple tissues during dorsal closure. *Curr. Biol.* **15**, 2208-2221.
García Fernández, B., Martinez Arias, A. and Jacinto, A. (2007). Dpp signalling orchestrates dorsal closure by regulating cell shape changes both in the amnioserosa and in the epidermis. *Mech. Dev.* **124**, 884-897.
Gorfinkiel, N. and Martínez Arias, A. (2007). Requirements for adherens junctions components in the interaction between epithelial tissues during dorsal closure in Drosophila. *J. Cell Sci.* **120**, 3289-3298.
Gorfinkiel, N., Blanchard, G. B., Adams, R. J. and Martinez-Arias, A. (2009). Mechanical control of global cell behaviour during dorsal closure in Drosophila. *Development* **136**, 1889-1898.
Grevengoed, E. E., Loureiro, J. J., Jesse, T. L. and Peifer, M. (2001). Abelson kinase regulates epithelial morphogenesis in Drosophila. *J. Cell Biol.* **155**, 1185-1198.
Harden, N. (2002). Signaling pathways directing the movement and fusion of epithelial sheets: lessons from dorsal closure in Drosophila. *Differentiation* **70**, 181-203.
Haviv, L., Brill-Karniely, Y., Mahaffy, R., Backouche, F., Ben-Shaul, A., Pollard, T. D. and Bernheim-Groswasser, A. (2006). Reconstitution of the transition from lamellipodium to filopodium in a membrane-free system. *Proc. Natl. Acad. Sci. USA* **103**, 4906-4911.
Homem, C. C. and Peifer, M. (2008). Diaphanous regulates myosin and adherens junctions to control cell contractility and protrusive behavior during morphogenesis. *Development* **135**, 1005-1018.
Howard, J. (2009). Mechanical signaling in networks of motor and cytoskeletal proteins. *Annu. Rev. Biophys.* **38**, 217-234.
Hutson, M. S., Tokutake, Y., Chang, M. S., Bloor, J. W., Venakides, S., Kiehart, D. P. and Edwards, G. S. (2003). Forces for morphogenesis investigated with laser microsurgery and quantitative modeling. *Science* **300**, 145-149.
Ingber, D. E. (2008). Tensegrity-based mechanosensing from macro to micro. *Prog. Biophys. Mol. Biol.* **97**, 163-179.
Jacinto, A. and Martin, P. (2001). Morphogenesis: unravelling the cell biology of hole closure. *Curr. Biol.* **11**, R705-R707.
Jacinto, A., Wood, W., Woolner, S., Hiley, C., Turner, L., Wilson, C., Martinez-Arias, A. and Martin, P. (2002). Dynamic analysis of actin cable function during Drosophila dorsal closure. *Curr. Biol.* **12**, 1245-1250.
Kaltschmidt, J. A., Lawrence, N., Morel, V., Balayo, T., Fernandez, B. G., Pelissier, A., Jacinto, A. and Martinez Arias, A. (2002). Planar polarity and actin dynamics in the epidermis of Drosophila. *Nat. Cell Biol.* **4**, 937-944.
Kiehart, D. P., Galbraith, C. G., Edwards, K. A., Rickoll, W. L. and Montague, R. A. (2000). Multiple forces contribute to cell sheet morphogenesis for dorsal closure in Drosophila. *J. Cell Biol.* **149**, 471-490.
Kim, Y. S., Fritz, J. L., Seneviratne, A. K. and VanBerkum, M. F. (2002). Constitutively active myosin light chain kinase alters axon guidance decisions in Drosophila embryos. *Dev. Biol.* **249**, 367-381.
Lamka, M. L. and Lipshitz, H. D. (1999). Role of the amnioserosa in germ band retraction of the Drosophila melanogaster embryo. *Dev. Biol.* **214**, 102-112.
Lecuit, T. and Lenne, P. F. (2007). Cell surface mechanics and the control of cell shape, tissue patterns and morphogenesis. *Nat. Rev. Mol. Cell Biol.* **8**, 633-644.
Ma, X., Lynch, H. E., Scully, P. C. and Hutson, M. S. (2009). Probing embryonic tissue mechanics with laser hole drilling. *Phys. Biol.* **6**, 036004.
Martin, A. C., Kaschube, M. and Wieschaus, E. F. (2009). Pulsed contractions of an actin-myosin network drive apical constriction. *Nature* **457**, 495-499.
Martin, A. C., Gelbart, M., Fernandez-Gonzalez, R., Kaschube, M. and Wieschaus, E. F. (2010). Integration of contractile forces during tissue invagination. *J. Cell Biol.* **188**, 735-749.
Martinez Arias, A. (1993). Development and patterning of the larval epidermis of Drosophila. In *The Development of Drosophila melanogaster*, vol. 1 (ed. A. Martinez Arias and M. Bate), pp. 517-607. Cold Spring Harbor, NY: Cold Spring Harbor Laboratory Press.
Mateus, A. M., Gorfinkiel, N. and Arias, A. M. (2009). Origin and function of fluctuations in cell behaviour and the emergence of patterns. *Semin. Cell Dev. Biol.* **20**, 877-884.
Oda, H. and Tsukita, S. (2001). Real-time imaging of cell-cell adherens junctions reveals that Drosophila mesoderm invagination begins with two phases of apical constriction of cells. *J. Cell Sci.* **114**, 493-501.
Paluch, E., Sykes, C., Prost, J. and Bornens, M. (2006). Dynamic modes of the cortical actomyosin gel during cell locomotion and division. *Trends Cell Biol.* **16**, 5-10.
Rauzi, M., Verant, P., Lecuit, T. and Lenne, P. F. (2008). Nature and anisotropy of cortical forces orienting Drosophila tissue morphogenesis. *Nat. Cell Biol.* **10**, 1401-1410.
Ricos, M. G., Harden, N., Sem, K. P., Lim, L. and Chia, W. (1999). Dcdc42 acts in TGF-beta signaling during Drosophila morphogenesis: distinct roles for the Drac1/JNK and Dcdc42/TGF-beta cascades in cytoskeletal regulation. *J. Cell Sci.* **112**, 1225-1235.
Riesgo-Escovar, J. R. and Hafen, E. (1997). Drosophila Jun kinase regulates expression of decapentaplegic via the ETS-domain protein Aop and the AP-1 transcription factor DJun during dorsal closure. *Genes Dev.* **11**, 1717-1727.
Rodriguez-Diaz, A., Toyama, Y., Abravanel, D. L., Wiemann, J. M., Wells, A. R., Tulu, U. S., Edwards, G. S. and Kiehart, D. P. (2008). Actomyosin purse strings: renewable resources that make morphogenesis robust and resilient. *HFSP J.* **2**, 220-237.
Royou, A., Sullivan, W. and Karess, R. (2002). Cortical recruitment of nonmuscle myosin II in early syncytial Drosophila embryos: its role in nuclear axial expansion and its regulation by Cdc2 activity. *J. Cell Biol.* **158**, 127-137.
Salbreux, G., Joanny, J. F., Prost, J. and Pullarkat, P. (2007). Shape oscillations of non-adhering fibroblast cells. *Phys. Biol.* **4**, 268-284.
Scuderi, A. and Letsou, A. (2005). Amnioserosa is required for dorsal closure in Drosophila. *Dev. Dyn.* **232**, 791-800.
Solon, J., Kaya-Copur, A., Colombelli, J. and Brunner, D. (2009). Pulsed forces timed by a ratchet-like mechanism drive directed tissue movement during dorsal closure. *Cell* **137**, 1331-1342.
Somogyi, K. and Rorth, P. (2004). Evidence for tension-based regulation of Drosophila MAL and SRF during invasive cell migration. *Dev. Cell* **7**, 85-93.
Strutt, D. I., Weber, U. and Mlodzik, M. (1997). The role of RhoA in tissue polarity and Frizzled signalling. *Nature* **387**, 292-295.
Wheeler, A. P. and Ridley, A. J. (2004). Why three Rho proteins? RhoA, RhoB, RhoC, and cell motility. *Exp. Cell Res.* **301**, 43-49.